Nanoscale

Accepted Manuscript

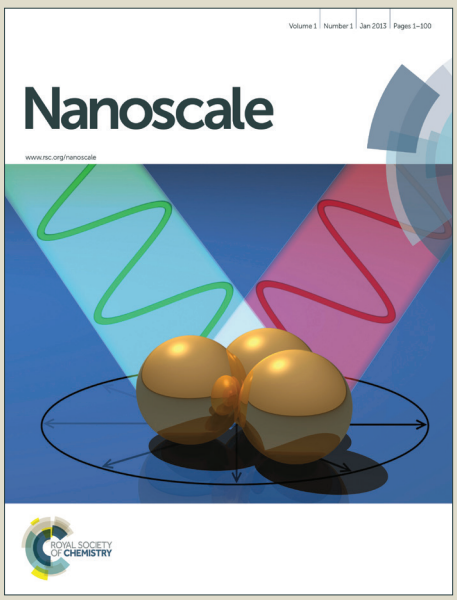

ROYAL SOCIETY OF CHEMISTRY

www.rsc.org/nanoscale

Patterning and tuning of electrical and optical properties of graphene by laser induced two-photon oxidation

Jukka Aumanen[1], *Andreas Johansson*[2]*, *Juha Koivistoinen*[1], *Pasi Myllyperkiö*[1], *Mika Pettersson*[1]*

[1]Nanoscience Center, Department of Chemistry, P.O. Box 35, FI-40014, University of Jyväskylä, Finland.

[2]Nanoscience Center, Department of Physics, P.O. Box 35, FI-40014, University of Jyväskylä, Finland

ABSTRACT

We demonstrate a simple all-optical patterning method for graphene, based on laser induced two-photon oxidation. By tuning the intensity and dose of irradiation, the level of oxidation is controlled, band gap is introduced and electrical and optical properties are continuously tuned. Complex patterning is performed for air-suspended monolayer graphene and for graphene on substrates. The presented concept allows development of all-graphene electronic and optoelectronic devices with an all-optical method.

Graphene has high potential for becoming the next generation material for electronics, photonics and optoelectronics.[1,2] Electrical properties of graphene can be modified by tuning its shape or dimension. Narrow ribbons of graphene lead to opening of a band gap due to quantum confinement effect. Patterning of ribbons has been achieved by nanolithographic methods and by self-organized growth.[3,4] However, creation of localized states due to disorder in nanoribbon edges is a problem.[5] More precise control of band gap has recently been achieved by bending graphene on a patterned SiC substrate leading to localized strain, but it is not clear how to make complex patterns from such structures.[6] Additionally, this method is limited to SiC substrates. Graphene oxide (GO) has a band gap, which can be tuned by controlling the degree of oxidation.[7,8] Patterning of GO by reduction using a heated AFM tip has been shown to increase conductivity by four orders of magnitude.[9] Pulsed laser induced reduction of GO in aqueous solution has been observed[10] and laser heating has been used for modification of electrical properties of GO.[11-14] However, thermal reduction of GO does not fully recover the excellent electrical properties of graphene. Laser-based ablation patterning of graphene has also been investigated.[15-19] Fabrication of sub-diffraction limited features, such as ribbons[15] has been demonstrated but formation of disordered edges makes it difficult to modify and control electrical properties. Here, we report patterning and controlled tuning of electrical and optical properties of graphene by femtosecond laser induced non-linear oxidation. The method relies on oxidation without ablation or cutting, thus the carbon network is preserved throughout the process. By tuning the level of oxidation, electrical properties of oxidized regions can be continuously fine-tuned; however, the excellent electrical properties of the non-oxidized regions of graphene are preserved.

We imaged patterns by four-wave mixing (FWM), which is a nonlinear optical method giving very strong response in nanomaterials.[20] Previously, we have used FWM to study individual single walled carbon nanotubes.[21] FWM signal of graphene was previously measured and an unusually large third order susceptibility, on the order of $|\chi^{(3)}| = 10^{-7}$ esu was obtained.[22] We used two input beams with wavelengths of 540 and 590 nm for FWM imaging, during which the sample chamber was purged with nitrogen.

Patterning was performed in ambient air using peak intensity of $10^{11} – 10^{12}$ W/cm^2. At higher intensities (>10^{12} W/cm^2), ablation of graphene took place. Laser patterning and FWM imaging of monolayer graphene, suspended over 7 x 7 μm^2 holes on copper TEM grid (Graphene Platform Corp.) are presented in Figure 1. The FWM signal is very strong and there is high contrast to the copper grid. Raman measurements for the sample showed characteristic features of monolayer graphene including higher intensity for the 2D band than for the G band (ESI Fig. S1).[23] In Figure 1A, a FWM image of graphene is shown before patterning and in Figures 1B – 1E images are shown after successive irradiation steps aimed at drawing a rectangular pattern. FWM signal from the pattern decreases after each irradiation step, showing that optical properties of graphene change. The patterned area forms a closed loop proving that patterning does not result in cutting, or ablation of graphene. This is a very important distinction to the previous laser patterning studies of graphene which relied on cutting and removal of material.[15-19] The sample was stored for three days at ambient conditions between images 1E and 1F, which shows that patterns are stable.

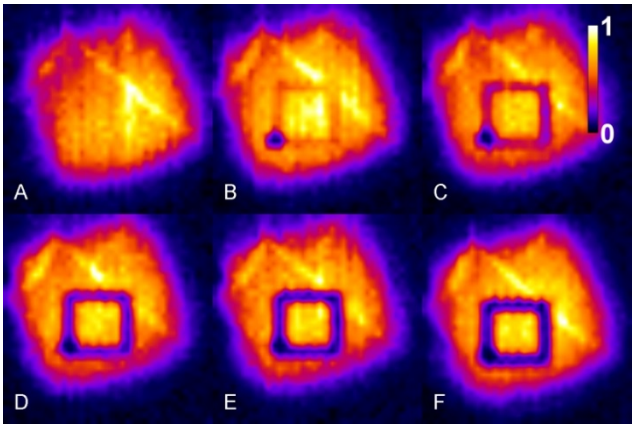

Figure 1. FWM images of patterned suspended monolayer graphene. The image shows the FWM signal strength at each pixel. (**A**) Before patterning. (**B – E**) Patterning at various stages of oxidation. (**F**) Image after storage of the sample for 3 days. The spot on the left lower corner is made in purpose in the early stage of patterning. The size of the laser patterned feature is approximately 2 x 2 μm^2. Graphene is suspended on the backside of the 4 μm thick copper grid which limits focusing of the beam to graphene surface near the edges of the square, thus the size of the FWM image of the graphene square is ~5 x 5 μm^2 although the actual size of the square is 7 x 7 μm^2.

Patterning did not occur under nitrogen purge, suggesting that the process involves oxidation of graphene by O_2. We studied patterning at different partial pressures of oxygen in oxygen/nitrogen mixtures which revealed that the rate of oxidation increases between 0 – 21 % of oxygen but not beyond that. (ESI Fig. S2). Figure 2 presents a FWM image of a sample where two square patches with a size of 2 x 2 μm^2 were patterned, using different irradiation times. Raman spectra measured from the patterned areas indicate that the G-band frequency shifts up and the D-band intensity increases upon irradiation (ESI Fig. S3), which are signatures

of oxidized graphene.[24] Raman measurement of non-patterned graphene was repeated after several hours of irradiation of the sample with Raman excitation laser. Changes were not observed in the spectrum proving that the oxidation does not occur by Raman excitation. In the lower panel of Figure 2, the G-band shift along a line marked in the FWM image is shown. The maximal shift is equal to ~13 cm^{-1}, which indicates substantial oxidation as the shift is similar to the observed G-band up-shift between pristine graphite and graphite oxide.[25] Another indication of strongly oxidized sample is that the intensity ratio of the D- and G-bands (I(D)/I(G)) increased from nearly zero in the non-irradiated area up to a value of 1.6 in the irradiated area (Figure 2). The I(D)/I(G) ratio is known to show values between 0.8 – 2.8 in GO and reduced graphene oxide (rGO), indicating possible differing functional group and/or oxygen contents.[26,27] Observation of characteristic Raman spectrum of oxidized graphene over an extended irradiated area, larger than the laser spot size, is another clear proof that no ablation or removal of material is taking place. In order to obtain further evidence of oxidation by laser irradiation, three areas of suspended monolayer graphene were irradiated and three control areas were left unexposed. Elemental analysis was performed for the areas using energy dispersive x-ray (EDX) analysis (ESI Fig. S4). O/C atomic ratio is on average 0.09 in the unprocessed areas and 0.22 in the processed areas, confirming oxidation by laser irradiation.

The mechanism of photo-oxidation was studied by measuring kinetics of the decay of the FWM signal at various laser powers for monolayer air-suspended graphene (ESI Fig. S5). Decay constant as a function of laser power squared is fitted with a linear function ($\chi^2 = 0.98$) indicating that the process involves two-photon absorption ($k \propto P^2$) (ESI Fig. S6). The effective two-photon cross-section, assuming 100 % quantum yield, for oxidation was obtained from the fit as 4 x 10^{-}

^{54} cm^4 s (ESI). This parameter is useful for designing patterning process with various lasers and for estimating the rate of patterning.

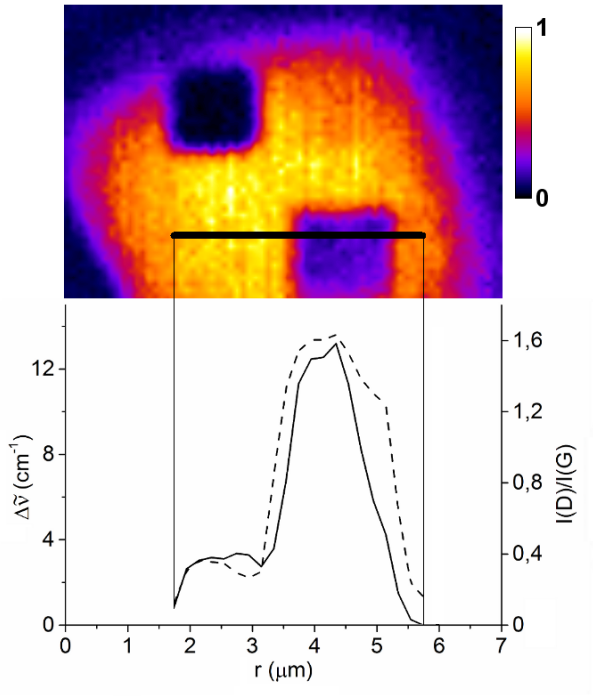

Figure 2. Upper panel: FWM image of a monolayer graphene sample where two rectangular patches were patterned using different irradiation times. Lower panel: Raman spectroscopic data along a line shown in the upper panel. Solid line (left axes) indicates the shift of the G-band from its value in non-irradiated graphene and the dashed line (right axis) indicates the value for the intensity ratio between the D-band and the G-band.

It is interesting to compare our results on photo-oxidation of graphene with previous studies of photoreduction of GO.[10-14] Photoreduction of GO is based on laser heating, which leads to detachment of oxygen containing groups similarly to reduction by hot AFM tip.[9] We use a very low average power, on the order of 10 μW, which cannot heat the sample significantly. Thus, our

method is not driven by laser heating but by a process involving excited state chemistry, which may explain why in our case irradiation leads to attachment of oxygen groups to graphene while previous studies on irradiation of GO led to opposite process.

We also patterned monolayer graphene on doped Si substrate with a 300 nm thick dielectric layer of silicon dioxide (SiO_2) (Graphenea). Figure 3 shows that features much below a micrometer can be drawn, arbitrary shapes including curved features can be made, the level of oxidation can be tuned and the oxidation level is stable over an extended area. The patterns are also visible by scanning electron microscopy (SEM) (Figure 3). The line width was determined from the SEM image of letter C (Figure 3, upper panel) yielding ~400 nm. For comparison, our microscope objective with a numerical aperture of 0.8 yields an estimated focal spot size of 430 nm at 540 nm wavelength. Two-photon excitation makes it effectively smaller by a factor of $2^{1/2}$ yielding ~300 nm, which is in reasonable agreement with the determined line width.

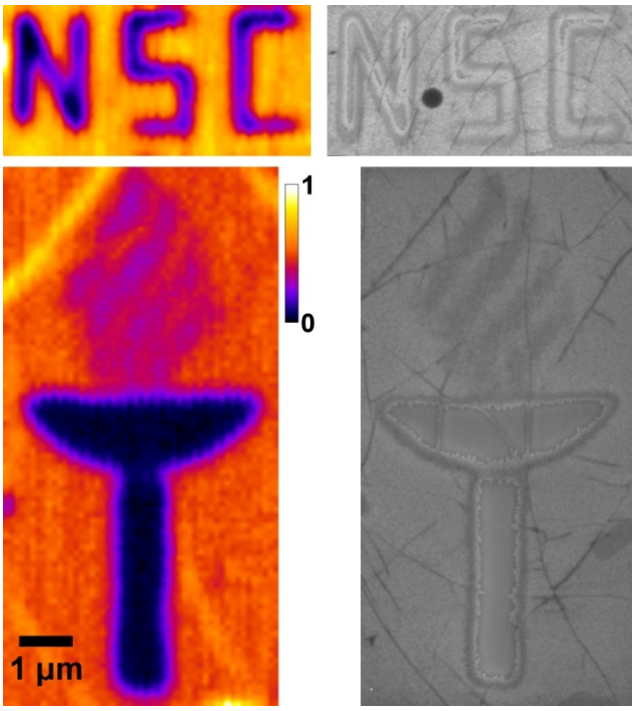

Figure 3. Patterns drawn on monolayer graphene on Si/SiO_2 substrate. FWM images are shown on the left and SEM images of the same patterns are shown on the right. The scale bar on the lower left corner applies to all panels.

Electrical properties of the patterned areas were studied. Metal electrodes were fabricated on the SiO_2 substrate and the graphene was etched into suitable shapes between the electrodes (upper inset of Figure 4A). In this structure, two neighbouring electrodes were selected and the I-V characteristics of that section were measured. The I-V curve was linear with a two-terminal conductance of 15 μS (Figure 4A). A line between the two electrodes was then gradually oxidized by repeated irradiations (upper inset of Figure 4A). The I-V curve was measured after each irradiation step and the results are presented in Figure 4A. The conductance of the graphene sample initially increased with 8.5 percent, after which it decreased gradually with more than 5 orders of magnitude. As the oxidation progressed, the I-V developed a nonlinear shape and at the

end turned non-conducting at low voltage bias. The data show the capability to gradually modify the electric properties of graphene through a conductor to insulator transition by changing its oxidation state.

Further evidence of tailoring of the electrical properties by laser patterning was obtained from using the doped Si chip as a back-gate to study the influence of a perpendicular electric field. For moderate laser exposures, when the I-V characteristics still remain linear, no observable change in conductance appears in the back-gate voltage range of -10 V to 10 V. At higher exposure doses, when the I-V has taken on a clearly non-linear shape, also back-gate dependence appears (Figure 4B). The graphene device acts as a p-type field-effect-transistor, with a current amplification of more than one order of magnitude at negative back-gate voltages. This demonstrates that the oxidation leads to opening of a band gap in the exposed region, which governs the electronic response.[28] A rough estimate of the band gap can be made from the current onset in the corresponding I-V curve (black trace in the inset of Figure 4B). By smoothing the noisy I-V curve (red trace) and then differentiating it, the onset appears as a peak in the resulting dI/dV curve (blue trace). The estimate gives a band gap in the range 310-580 meV, due to the I-V not being fully symmetric. This initial result is very promising, considering that in the present case contact resistance is relatively high and the graphene includes grain boundaries. Both these factors suppress the ON-state current, and give reason to believe the ON/OFF ratio of 10 can be significantly improved.

In summary, we presented a novel all-optical method for patterning graphene. We used femtosecond pulses to induce oxidation in irradiated areas via two-photon mechanism. The patterned areas were imaged by FWM with high sensitivity. Electronic measurements showed

that oxidation leads to opening of a band gap in graphene. The results of this work will allow development of all-graphene electrical devices and other applications of graphene.

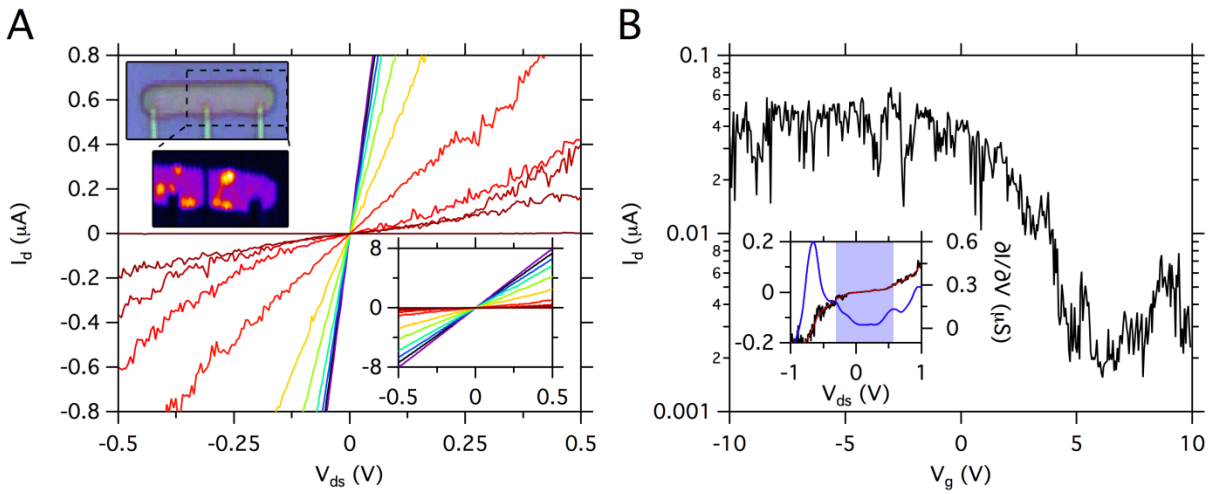

Figure 4. Electronic measurements at different oxidation states. (**A**) Drain current versus applied drain-source voltage, taken before two-photon oxidation (black) and in between oxidation steps (rainbow colors, purple through dark red). The data range captures the change from linear to non-linear I-V characteristics. Upper left inset: Upper pane shows optical image of sample geometry. Distance between electrodes is 6 μm. Lower pane shows a FWM image after the oxidation line is made. Lower right inset: I-V characteristics, displaying the upper range of conductance variation with linear response. (**B**) Current versus gate voltage at a fixed V_{ds} of 100 mV, displaying p-type transfer characteristics. Inset: Corresponding non-linear I-V characteristics (black), the I-V after smoothing (red), and differentiation of the latter trace (blue). The light blue shaded region from -310 mV to 580 mV marks the highly resistive plateau in the I-V trace.

Electronic Supplementary Information (ESI) available: Detailed procedures of FWM imaging, photo-oxidation, Raman spectroscopy, SEM-EDX measurements, sample fabrication,

and electronic measurements; calculation of the two-photon cross-section for oxidation; and Figures S1-S6.

Corresponding Author

*E-mail: mika.j.pettersson@jyu.fi

*E-mail: Andreas.johansson@jyu.fi.

ACKNOWLEDGMENTS

This work was funded by the Academy of Finland (decision. no. 252468). Janne Ihalainen is thanked for discussions. Hannu Salo is thanked for assistance with EDX measurements.

REFERENCES

1. P. Pasanen, M. Voutilainen, M. Helle, X. Song and P. J. Hakonen, *Phys. Scr.,* 2012, **T146**, 014025.

2. Q. Bao and K. P. Loh, *ACS Nano,* 2012**, 6,** 3677 – 3694.

3. C. Berger, Z. Song, X. Li, X. Wu, N. Brown, C. Naud, D. Mayou, T. Li, J. Hass, A. N. Marchenkov, E. H. Conrad, P. N. First and W. A. de Heer, W. A., *Science,* 2006, **312,** 1191–1196.

4. M. Sprinkle, M. Ruan, Y. Hu, J. Hankinson, M. Rubio-Roy, B. Zhang, X. Wu, C. Berger and W. A. de Heer, *Nature Nanotech.,* 2010, **5,** 727–731.

5. M. Han, J. C. Brant and P. Kim, *Phys. Rev. Lett.,* 2010, **104,** 056801.

6. J. Hicks, A. Tejeda, A. Taleb-Ibrahimi, M. S. Nevius, F. Wang, K. Shepperd, J. Palmer, F. Bertran, P. Le Fevre, J. Kunc, W. A. de Heer, C. Berger, and E. H. Conrad, *Nature Phys.*, 2013, **9,** 49–54.

7. I. Jung, D. A. Dikin, R. D. Piner and R. S. Ruoff, *Nano Lett.* 2008, **8,** 4283–4287.

8. J.-A.Yan, L. Xian and M. Y. Chou, *Phys. Rev. Lett.*, 2009, **103,** 086802.

9. Z. Wei, D. Wang, S. Kim, S.-Y. Kim, Y. Hy, M. K. Yakes, A. R. Laracuente, Z. Dai, S. R. Marder, C. Berger, W. P. King, W. A. de Heer, P. E. Sheehan and E. Riedo, *Science*, 2010, **328,** 1373–1376.

10. V. Abdelsayed, S. Moussa, H. M. Hassan, H. S. Aluri, M. M. Collinsson, M. S. El-Shall. *J. Phys. Chem. Lett.* 2010, **1**, 2804 – 2809.

11. Y. Zhou, Q. Bao, B. Varghese, L. A. I. Tang, C. K. Tan, C.-H. Sow and K. P. Loh, *Adv. Mater.*, 2010, **22,** 67–71.

12. Y. Zhang, L. Guo, S. Wei, Y. He, H. Xia, Q. Chen, H.-B. Sun and F.-S. Xiao, *Nano Today*, 2010, **5,** 15–20.

13. V. Strong, S. Dubin, M. F. El-Kady, Y. Wang, B. H. Weiller and R. B. Kaner, *ACS Nano*, 2012, **6,** 1395–1403.

14. L. Guo, R.-Q. Shao, Y.-L. Zhang, H.-B. Jiang, X.-B. Li, S.-Y. Xie, B.-B. Xu, Q.-D. Chen, J.-F. Song and H.-B. Sun, *J. Phys. Chem. C*, 2012, **116,** 3594–3599.

15. R. J. Stöhr, R. Kolesov, K. Xia and J. Wrachtrup, *ACS Nano*, 2011, **6,** 5141–5150.

16. W. Zhang, Z. B. Wang, A. A. Pena, D. J. Whitehead, M. L. Zhong and H. W. Zhu, *Appl. Phys. A,* 2012, **109,** 291–297.

17. V. Kiisk, T. Kahro, J. Kozlova, L. Matisen and H. Alles, *Appl. Surf. Sci.*, 2013, **276,** 133–137.

18. J.-H. Yoo, J. B. Park, S. Ahn and C. P. Grigoropoulos, *Small*, 2013, **9,** 4269–4275.

19. R. Sahin, E. Simsek and S. Akturk, *Appl. Phys. Lett.*, 2014, **104,** 053118.

20. Y. Wang, C.-Y. Lin, A. Nikolaenko, V. Raghunathan and E. O. Potma, *Adv. Opt. Photon.*, 2011, **3,** 1–52.

21. P. Myllyperkiö, O. Herranen, J. Rintala, H. Jiang, P. R. Mudimela, Z. Zhu, A. G. Nasibulin, A. Johansson, E. I. Kauppinen, M. Ahlskog and M. Pettersson, *ACS Nano*, 2010, **4,** 6780–6786.

22. E. Hendry, P. J. Hale, J. Moger, A. K. Savchenko and S. A. Mikhailov, *Phys. Rev. Lett,* 2010, **105,** 097401.

23. Z. Ni, Y. Wang, T. Yu and Z. Shen, *Nano Res.*, 2008, **1,** 273–291.

24. G. Eda and M. Chowalla, *Adv. Mater.*, 2010, **22,** 2392–2415.

25. S. Stankovich, D. A. Dikin, R. D. Piner, K. A. Kohlhaas, A. Kleinhammes, Y. Jiac, Y. Wuc, S. T. Nguyenb and R. S. Ruoffa, *Carbon,* 2007, **45,** 1558–1565.

26. D. S. Sutar, P. K. Narayanam, G. Singh, V. D. Botcha, S. S. Talwar, R. S. Srinivasa and S. S. Major, *Thin Solid Films,* 2012, **520,** 5991–5996.

27. T. V. Cuonga, V. H. Phama, Q. T. Tranb, S. H. Hahn, J. S. Chung, E. W. Shin and E. J. Kim, *Mater. Lett.*, 2010, **64,** 399–401.

28. A. Nourbakhsh, M. Cantoro, T. Vosch, G. Pourtois, F. Clemente, M. H. van der Veen, J. Hofkens, M. M. Heyns, S. De Gendt and B. F. Sels, *Nanotechnol.*, 2010, **21,** 435203.

TABLE OF CONTENTS ENTRY

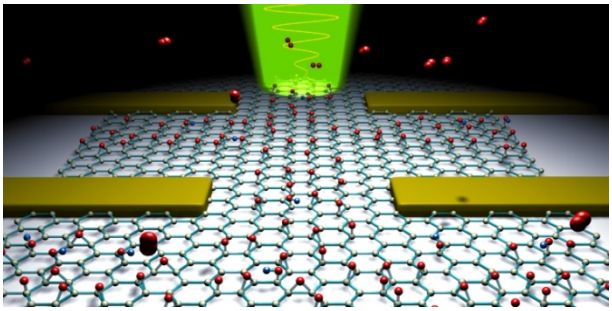

Laser-induced two-photon oxidation modifies locally the electrical and optical properties of monolayer graphene allowing optical fabrication of all-graphene devices.